Enhanced Power Handling and Quality Factor in Thin-Film Piezoelectric-on-Substrate Resonators

Reza Abdolvand*, and Farrokh Ayazi
School of Electrical and Computer Engineering
Georgia Institute of Technology, Atlanta, GA 30332
Email: reza.abdolvand@okstate.edu; ayazi@ece.gatech.edu
* now an assistant professor at Oklahoma State University (School of ECE), Stillwater, OK 74078

***Abstract*— In this paper, we report on the superior quality factor and power handling of thin-film piezoelectric-on-substrate (TPoS) resonators. A maximum *Q* of 17000 in vacuum is measured for an AlN-on-Silicon resonator at ~35MHz, and a maximum *f.Q* product of ~2.9x10^{12} is measured in air for a device resonating at 500MHz. AlN-on-Silicon resonators are fabricated on a 10µm thick SOI substrate where the AlN film is 1µm thick. The quality factor and the power handling are measured and compared before and after removing the structural silicon layer from the backside of a resonator. The measured results verify the advantages of including a silicon substrate in the resonant structure for oscillator applications.**

Keywords- thin-film piezoelectric; quality factor; power handling; oscillator

I. INTRODUCTION

Micromachined lateral-bulk-acoustic resonators (LBAR) are of great interest where multi-frequency references and clock signals are desired on a single chip. High quality factor and enhanced linearity improve the phase-noise of the oscillator built using these resonators, while small motional impedance reduces the required loop-gain and hence the power consumption [1]. Although capacitively-transduced single crystal silicon resonators exhibit excellent *Q* values [2], they suffer from nonlinear nature of the capacitive transducer [3] and their motional impedance escalates rapidly to very large values with frequency. Thin-film piezoelectric resonators on the other hand, outperform capacitive micro-resonators in motional impedance as a result of the inherently large electromechanical coupling of the piezoelectric transduction [4]. However, the reported quality factor in these devices is relatively low and the limited thickness of the resonant body places a constraint on their linearity.

In this work, thin-film piezoelectric-on-substrate (TPoS) resonators [5] are studied and verified to exhibit excellent linearity and high quality factors while maintaining low motional impedance in small footprints. The device layer of a silicon-on-insulator (SOI) substrate forms the bulk of the resonant structure in the devices investigated in this work. Therefore, the improvements in the resonator performance can be related to the superior acoustic properties (low loss, high energy density) of single crystal silicon.

As a result of improved nonlinearity in a TPoS resonator signal power can be increased in the sustaining loop of an oscillator built with the resonator. Therefore, signal to noise ratio is increased and the phase-noise is consequently reduced. The enhanced far-from-carrier phase-noise of a ~106MHz TPoS-based oscillator presented in this work compared to oscillators based on capacitive resonators at the same frequency range [2] validates the advantages of TPoS resonators.

This work was supported by National Science Foundation.

II. TPOS RESONATOR STRUCTURE

A TPoS resonator is comprised of a thin piezoelectric layer sandwiched between two metallic electrodes stacked on top of a relatively thick (>2µm) layer of low-acoustic-loss material (such as single crystal silicon or nanocrystalline diamond). The resonant structure is released from the rest of the substrate and it is suspended by anchors placed around the resonator edge at the nodal points of a targeted resonance mode shape (Fig. 1).

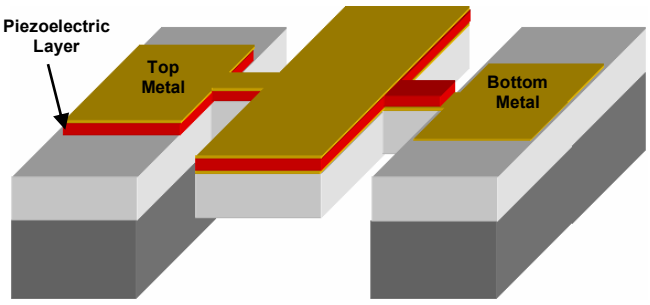

Figure 1: The schematic structure of a one-port TPoS resonator.

The typical resonator shown above is an example of a one-port TPoS block resonator. Metal electrodes in a TPoS resonator can alternatively be split into electrically isolated pairs to form two-port resonators. The resonator geometry and the metal electrode patterns determine the main excited resonance mode as well as the resonance frequency. High-order lateral-extensional modes of a block resonator can be excited by patterning the top electrode in an interdigitated finger configuration [6].

III. NONLINEARITY IN TPOS RESONATORS

The smaller size of micromechanical resonators, despite all of the advantages has an inevitable drawback when it comes to the maximum allowable stored energy or in other word power handling. Power handling is a measure of the amount of power that can be applied to or delivered by the resonator. The power

handling is mostly limited by different nonlinearity mechanisms in the resonator. In piezoelectric resonators the conversion of the applied electric field to stress is governed by a linear equation in the most part. Therefore, the effective source of nonlinearity is the nonlinear stiffness of the resonant structure which gives rise to the dependency of the resonance frequency on the vibration amplitude. This nonlinearity will introduce noise and distortion in the output signal of an oscillator [7] and the oscillation power should be kept less than the nonlinear limits at all times.

In order to study the power handling limits in a resonator we begin with rewriting the nonlinear spring coefficient as:

$$k = k_0(1 + k_1 x + k_2 x^2 + ...) \quad (1)$$

where k_1, k_2, ... are nonlinear spring constants. A nonlinear spring coefficient will cause higher harmonics of the natural resonance frequency to appear in the output. Consequently, the resonance frequency (frequency at which the largest vibration amplitude occurs) is dependent on the vibration amplitude predicted by the equation below [8]:

$$\omega_{nonlinear} = \omega_0(1 - \frac{5k_1^2}{12} A + \frac{3k_2}{8} A) \quad (2)$$

where ω_0 is the linear resonance frequency and A is the vibration amplitude. From the above expression it is identified that a non-zero first-order nonlinear spring coefficient (k_1) will shift down the resonance frequency and the second-order nonlinear coefficient (k_2) will shift the frequency either up or down depending on its sign. It can be assumed that the limit for largest allowable vibration amplitude (x_c) is the bifurcation point (the critical point after which the amplitude versus frequency plot will demonstrate hysteresis) (Fig. 2).

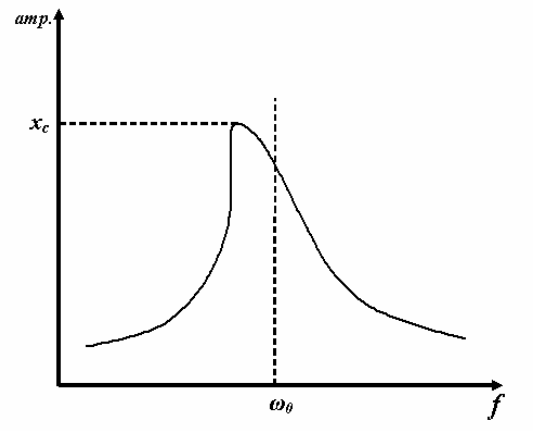

Figure 2: A frequency response plot of a resonator operating at bifurcation.

By incorporating the maximum allowable vibration amplitude, the maximum stored energy in the resonator can be calculated from:

$$E_{max} = \frac{1}{2} k_0 x_c^2 \quad (3)$$

It is clear from the above analysis that the maximum stored energy or in other word the power handling of a resonator is directly proportional to the effective stiffness of the resonant structure which in turn is proportional to the thickness in a block structure such as Fig. 1 resonating in lateral-extensional resonance mode. Needless to say, smaller nonlinear spring coefficient increases the power handling. Nonlinear spring coefficients are dictated by material properties and vary for each material of choice. To compare the nonlinearity limitations in different material a normalized parameter called energy density is defined as the maximum allowable energy divided by the volume of the resonant structure. Silicon resonators exhibit orders of magnitude larger energy density than piezoelectric material such as quartz [8].

Considering the above analysis we can conclude that the advantage of including a relatively thick silicon substrate in the resonant body of a TPoS resonator is two-fold; first it increases the stiffness and eventually increases the energy density, and second, silicon in inherently a very high energy density material and therefore linearity is expected to further improve. Measurement results presented in the following chapters agree with this conclusion.

IV. AlN-on-Silicon Resonators

The SEM of Fig. 3 presents a typical third-order AlN-on-silicon resonator utilized in this work. The fabrication process flow is mostly the same as what was introduced in the prior work [5]. The starting substrate is a 10μm SOI. The thickness of the sputtered AlN is 1μm and it is deposited on a 100nm thick Mo bottom electrode. The top electrode is made of a 100nm thick aluminum layer and it is patterned using lift-off process. To define the resonator structure the AlN layer is etched in an inductively coupled plasma (ICP) chamber using Cl_2 gas. The silicon layer is etched in an ICP chamber using Bosch recipe. Finally the device is released from the backside by dry-etching the silicon handle and the buried oxide layers in ICP chambers.

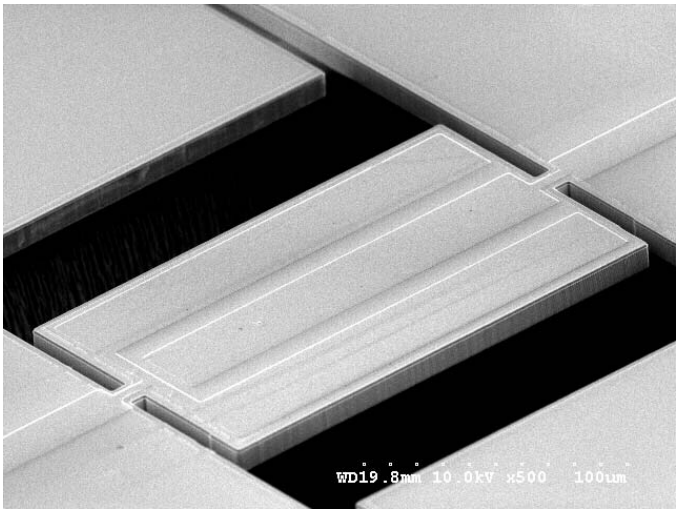

Figure 3: The SEM of a third-order AlN-on-Silicon TPoS resonator.

A. Frequency Response Measurement

The top electrode pattern in high-order TPoS resonators matches with the strain field developed in the structure at resonance to maximize the coupling coefficient for that mode.

However, fundamental resonance mode of the structure can always be excited in this configuration as well.

All measurements in this work are performed on a Suss high-frequency probe station using Agilent E8364B network analyzer and Cascade GSG probes. A Lakeshore vacuum probe-station connected to an Agilent E5071B network analyzer is also used for performing the measurements under vacuum.

Frequency response plot (S_{21}) shown in Fig. 4 is measured in air from a device simillar to the one show in Fig. 3 and resonating in the fundamental mode. The motional impedance of the device is 350Ω @36MHz and the unloaded Q is ~10000 (considering 50Ω termination resistance).

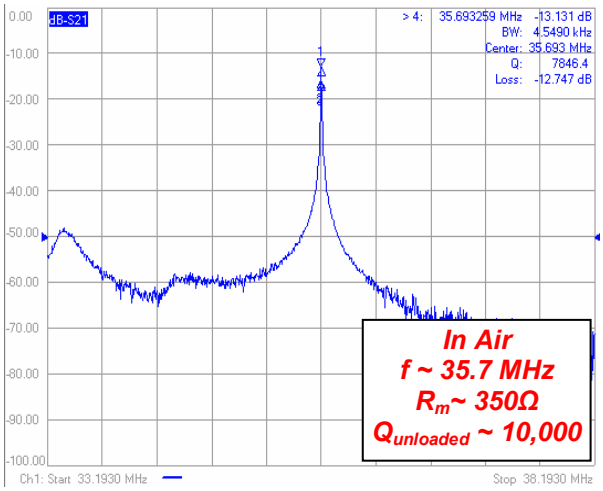

Figure 4: The frequency response plot (S_{21}) measured in air from the device shown in Fig. 3 at fundamental mode.

The measurement is repeated in vacuum for the same device and the result is shown in Fig. 5. The unloaded quality factor is increased to ~17000 and the motional impedance is inversely reduced to 180Ω.

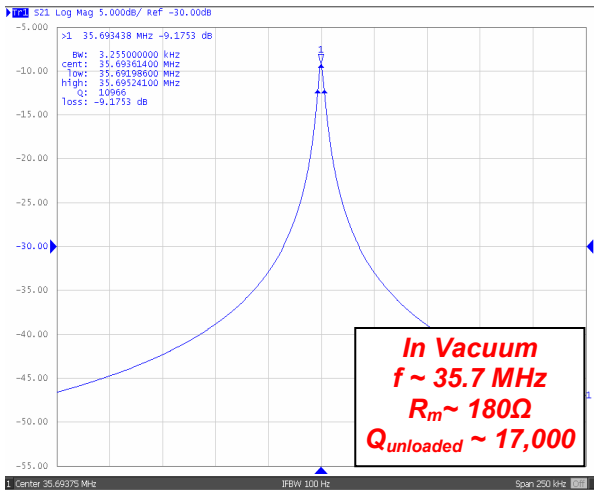

Figure 5: The frequency response plot (S_{21}) measured in vacuum from the device shown in Fig. 3 at fundamental mode.

The third-order resonance mode of the same device is measured at ~106MHz with $Q_{unloaded}$ ~ 8000 in air. The resonance frequency of these resonators can be increased by reducing the finger pitch size of the top electrode. Moreover, the motional impedance can be reduced by increasing the mode-number.

The frequency response shown in Fig. 6 is measured from a ninth-order AlN-on-silicon device with 10μm finger pitch size (inset SEM). The motional impedance of this device is ~70Ω @208MHz and the unloaded Q is ~6000.

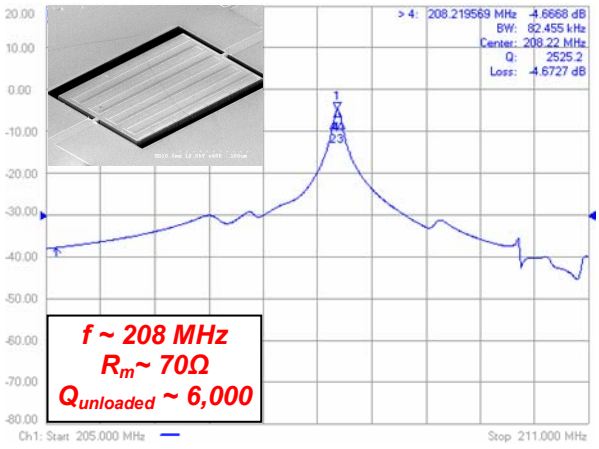

Figure 6: The frequency response plot (S_{21}) measured in air from a ninth-order AlN-on-silicon resonator (inset SEM).

The highest $f \cdot Q$ product (2.9×10^{12}) is measured from a 500MHz resonator with an unloaded Q of ~5800 in air (Fig. 7). The quality factor of these high frequency devices is not improved significantly while tested in vacuum.

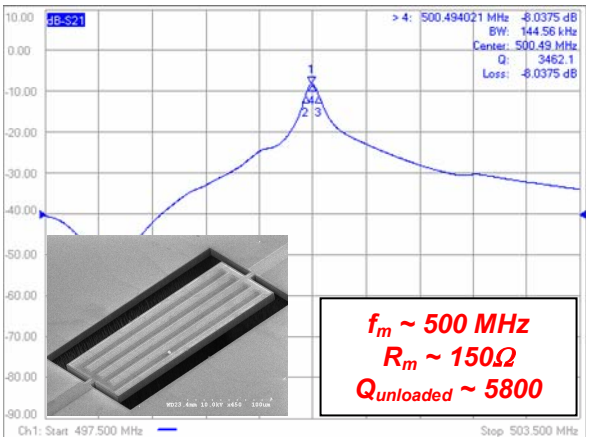

Figure 7: The frequency response plot (S_{21}) measured in air from a 500MHz AlN-on-silicon resonator.

The Q values presented in this work are higher than the measured values from lateral piezoelectric devices reported before. Since in these devices the acoustic energy is mostly confined in the single crystal silicon body of the resonator the improvement in the quality factor can be attributed to the low acoustic loss of silicon substrate.

B. Nonlinearity Measurement

The frequency response of a device similar to the one shown in Fig. 3 is measured in air at several input power levels ranging from -15dBm to 10dBm. Results for -15dBm and 10dBm applied powers are overlapped and plotted in Fig. 8. As

seen in the figure the change in the response is very minute and the resonance peak is slightly shifted toward lower frequencies for higher input power.

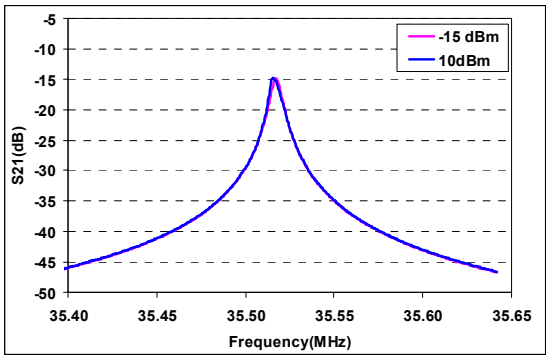

Figure 8: Overlapped frequency response plots (S_{21}) measured in air from the AlN-on-silicon resonator of Fig. 3 with two different input power levels.

In order to better understand the effect of the silicon substrate layer on the linearity of the resonator, frequency response measurements for the same device are repeated after etching the silicon layer from the backside of the device. Results are plotted in Fig. 9.

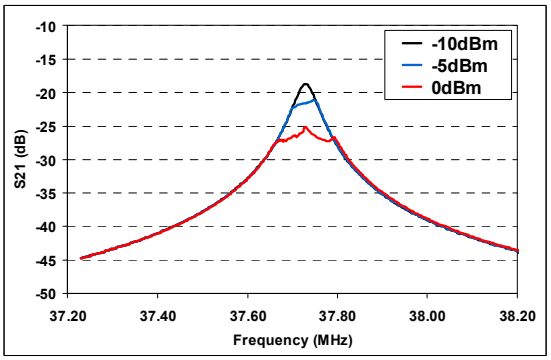

Figure 9: Overlapped frequency response plots measured from the AlN-on-silicon resonator of Fig. 3 after etching the silicon layer from the backside.

As expected, the resonance frequency after etching the silicon layer is slightly increased, since the acoustic velocity in AlN is higher than acoustic velocity in silicon. On the other hand, the resonator exhibit highly nonlinear behavior starting from -10dBm of input power. The measured quality factor of the resonator is also reduced from ~6000 to less than a 1000 after etching the silicon layer. This observation can clearly confirm the advantages of including the silicon substrate in a lateral-extensional resonator.

V. Oscillator Phase-Noise

In order to further study the effect of improved linearity of a TPoS resonator in oscillator applications a single-transistor transimpedance amplifier (TIA) [5] is connected to the resonator of Fig. 3 in a loop. The phase-noise performance of the oscillator is measured and recorded. Next, the same resonator is connected to a CMOS TIA chip [1] and the phase noise measurement is repeated. The power consumption in the CMOS TIA is 4× larger than the simple single-transistor configuration and the oscillation power is higher. Phase-noise results are plotted in Fig. 10.

As seen the phase-noise performance of the oscillator is improved and the far-from-carrier phase-noise is reduced to ~ −147dBc/Hz. Unlike the oscillator circuits based on capacitive resonators [2], there is no automatic level control (ALC) unit in the sustaining circuit of this TPoS oscillator.

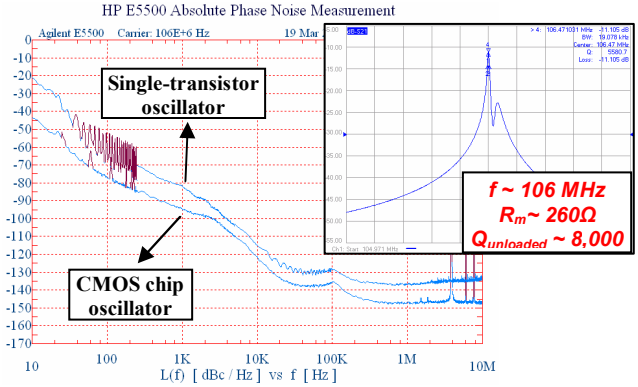

Figure 10: Overlapped phase-noise plots measured from a 106MHz oscillator with two different sustaining circuits and the frequency response of the utilized AlN-on-silicon resonator.

Acknowledgment

The authors would like to thank Hossein Mirilavasani for his contribution in the oscillator design and measurement, and the staff at Microelectronic Research Center at Georgia Tech.

References

[1] H. M. Lavasani, R. Abdolvand, and F. Ayazi, "A 500MHz low phase-noise AlN-on-silicon reference oscillator," *in Proc. IEEE CICC*, pp. 599-602, Sep. 2007.

[2] K. Sundaresan, G.K. Ho, S. Pourkamali, F. Ayazi, "A low phase noise 100MHz silicon BAW reference oscillator," *IEEE Custom Integrated Circuits Conference*, pp.841-844, 10-13 Sept. 2006.

[3] V. Kaajakari, J.K. Koskinen, T. Mattila, "Phase noise in capacitively coupled micromechanical oscillators," *IEEE Transactions on Ultrasonics, Ferroelectrics and Frequency Control,* vol.52, no.12, pp. 2322-2331, Dec. 2005.

[4] G. Piazza, P. J. Stephanou, A. P. Pisano, "Piezoelectric aluminum nitride vibrating contour-mode MEMS resonators," *Journal of Microelectromechanical Systems,* vol.15, no.6, pp.1406-1418, Dec. 2006.

[5] R. Abdolvand, H. Mirilavasani, F. Ayazi, "A low-voltage temperature-stable micromechanical piezoelectric oscillator," *International Conference on Solid-State Sensors, Actuators and Microsystems (TRANSDUCERS'07)*, pp.53-56, 10-14 June 2007.

[6] G. K. Ho, R. Abdolvand, and F. Ayazi, "High Order Composite Bulk Acoustic Resonators," *Proc. 20th IEEE International Conference on Micro Electro Mechanical Systems (MEMS 2007)*, Kobe, Japan, pp. 791-794, Jan 2007.

[7] J.J. Gagnepain, M. Oliver, F.L. Walls, "Excess Noise in Quartz Crystal Resonators," *37th Annual Symposium on Frequency Control*, pp. 218-225, 1983.

[8] V. Kaajakari, T. Mattila, A. Oja, H. Seppa, "Nonlinear limits for single-crystal silicon microresonators," *Journal of Microelectromechanical Systems,*vol.13, no.5, pp. 715-724, Oct. 2004.